Pérez, JJ.; D'avila, A.; Aryana, A.; Trujillo Guillen, M.; Berjano, E. (2016). Can Fat Deposition After Myocardial Infarction Alter the Performance of RF Catheter Ablation of Scar-Related Ventricular Tachycardia?: Results from a Computer Modeling Study. Journal of Cardiovascular Electrophysiology. 27(8):947-952. doi:10.1111/jce.13006.

Can fat deposition after myocardial infarction alter the performance of RF catheter ablation of scar-related ventricular tachycardia?

Results from a computer modeling study

Juan J. Pérez, MS, PhD[1], Andre d'Avila, MD, PhD[2], Arash Aryana, MS, MD, FHRS[3], Macarena Trujillo, MS, PhD[4], and Enrique Berjano, MS PhD[5]

From [1]Centro de Investigación e Innovación en Bioingeniería (Ci2B), [4]Instituto Universitario de Matemática Pura y Aplicada, [5]Biomedical Synergy, Electronic Engineering Department, Universitat Politècnica de València, Valencia, Spain, [2]IPAC- Instituto de Pesquisa em Arritmia Cardiaca - Hospital Cardiologico, Florianopolis – SC, Brazil, and [3]Dignity Health Heart and Vascular Institute, Sacramento, CA, USA

Word count: 2,750

Corresponding author: Dr. Enrique Berjano, Electronic Engineering Department (Building 7F), Universitat Politècnica de València, Camino de Vera, 46022 Valencia, Spain; Phone: 34–963877607, Fax: 34–963877609; Email: eberjano@eln.upv.es

Financial support: This work was supported by the Spanish "Plan Estatal de Investigación, Desarrollo e Innovación Orientada a los Retos de la Sociedad" under Grant TEC2014-52383-C3 (TEC2014-52383-C3-1-R).

Abstract

Introduction: The outcomes of catheter ablation of scar-mediated ventricular tachycardia (VT) remain far from perfect. Presence of fat as a component of the underlying substrate for scar-mediated VT could be relevant since this entity can seriously impede the passage of RF current due to its low electrical conductivity.

Methods and Results: Computer models of RF ablation were built in order to investigate the means by which the spatial heterogeneity of different tissues represented within the ventricular infarct zone, including the viable myocardium, fibrous tissue and fat could influence temperature distributions during RF ablation. The results demonstrated that spatial distributions of different tissue types significantly alter the density of electrical current largely as a result of fat impeding the passage of current. However, the thermal lesions appear minimally unaffected by this phenomenon, with variations in depth of ~1 mm.

Conclusion: While during RF ablation of scar-related ventricular tachycardia differences in tissue characteristics may affect the density of electrical current on a small-scale, overall this does not appear to significantly impact the size of the created thermal lesions.

Key Words: computer model, fat deposition, myocardial infarction, RF ablation, scar-related ventricular tachycardia

Introduction

The outcomes of catheter ablation of scar-mediated ventricular tachycardia (VT) remain far from perfect.[1] The quality of the ablation lesions delivered to the VT substrate is likely one of the most important factors determining the clinical outcome. One reason may be that radiofrequency (RF) energy represents a suboptimal energy modality for catheter ablation of scar tissue. Yet, experimental studies suggest that presence of scar by itself does not significantly impact lesion size or intramural temperatures reached in the cardiac tissue during RF ablation.[2-4] However, in these studies RF ablation was performed 1–4 months after creating the infarct model, not taking into account the impact of fat deposition which is typically encountered much later in regions of chronic myocardial infarction[5-7] coexisting with areas of fibrosis that together form the underlying substrate for reentrant VT.[8] Presence of fat as a component of the underlying substrate for scar-mediated VT is indeed relevant since this entity can seriously impede the passage of RF current due to its low electrical conductivity.[9] However, it would be difficult to experimentally evaluate the means through which fat and its spatial dispersion throughout the infarct zone could impact temperature distributions during RF ablation. In this regard, computer modeling can serve as a valuable tool to allow assessment and evaluation of various elements that can influence RF ablation in such a setting.[10] Computer models are based on physical equations which describe well-known electrical and thermal phenomena occurring during RF ablation. The aim of this computational study is to investigate the means by which the spatial heterogeneity of different tissues represented within the ventricular infarct zone, including the viable myocardium, fibrous tissue and fat could influence temperature distributions during RF ablation.

Methods

We created computer models of human ventricular tissue (wall thickness: 7 mm) with associated epicardial fat (2 mm thick) and connective tissue. The ventricular wall was comprised of 3 tissue types – viable myocardium, fibrous tissue, and fat – following a spatial distribution based on a microscopic image reported by Sasaki et al[5] (see Fig. 1A). The volume of modeled ventricular wall was built by rotating this image over a symmetry axis as shown in Fig. 1B. We considered a 60-s ablation conducted with a 7-Fr 3.5-mm length irrigated electrode placed perpendicularly on the endocardium (0.76 mm insertion depth). Fig. 1C shows an overview of the model showing the electrode surrounded by blood, the ventricular wall placed on the epicardial fat layer, which was placed on a fragment of connective tissue. The dispersive electrode was assumed to be on the bottom surface. The temperature distribution within the tissue was obtained by solving the Bio-heat equation.[11] Table 1 shows the physical characteristics of the tissues and materials employed in this model.[10,12,13] The irrigated electrode was modeled by fixing a value of 45ºC in the cylindrical zone of the electrode tip, and leaving the semispherical tip free.[10] The circulating blood in the ventricle was also included in the model, and its thermal effect was modeled with thermal transfer coefficients between blood and the tissue (h_T= 610 W/m^{2}K) and between blood and the electrode (h_E= 3,346 W/m^{2}K).[13] Blood perfusion into the tissue was irreversibly ceased once tissue temperature reached 50ºC. Both the initial temperature and the temperature for the surfaces away from the active electrode were initially assumed to be 36 ºC. The ANSYS program (ANSYS, Canonsburg, PA, USA) was used for creation of the Finite Element Model and the computer simulations. Convergence tests were conducted to

obtain the optimal outer dimensions of the model (shown in Fig. 1C) and meshing size (20-50 microns into the ventricular wall, shown in Fig. 1B).The models had around 240,000 elements and 120,000 nodes. The time-step was automatically set by ANSYS, from 2 ms at the beginning of the ablation until 0.1 s at the end.

We first assessed computationally the temperature distributions reached in the different types of tissue. Next, we examined through additional computer simulations as to how certain alterations in the spatial distribution of the 3 tissue types could influence lesion geometry. The lesion geometry was assessed by means of the 50ºC isotherm.[13] In comparison, we also simulated a control case in which the ventricular wall was comprised exclusively of viable myocardium. As such, we were able to quantify the potential impact of the 3 tissue types on lesion geometry itself.

Additionally, we also constructed computer models to mimic the experiment models created by Kottkamp et al[2] comparing tissue temperature progress during RF catheter ablation (RFCA) in chronic myocardial infarction versus normal myocardium. To replicate the proposed ex vivo conditions, we considered a constant temperature 60-s ablation (target: 80ºC) delivered using a 7-Fr 4-mm non-irrigated electrode placed perpendicularly on the endocardium (0.4 mm insertion depth). Also consistent with the proposed model, temperature progress was measured at 2 points: 3 mm (subendocardial position) and 6 mm (intramural position) from the tissue surface. The effects of forced thermal convection at the endocardium–blood and the electrode–blood interfaces were taken into account using a thermal transfer coefficient. Meanwhile, since no flow around electrode was setup,[2] we considered a coefficient of 500 W/m^2K, which corresponds to a typical value for natural convection between solid and liquid. Kottkamp et al found that the infarcted zone was

characterized by collagen, connective tissue and surviving myocardial muscle fibers.[2] Since they used a 15–24 days–old infarction model, it can be assumed that fat was not present. To build a computer model compatible with the experimental conditions used by Kottkamp et al, we considered the electrical characteristic reported by Salazar et al[14] using the transmural measurement method at 316 kHz. These authors reported a range of possible values for electrical conductivity of 0.44 – 0.75 S/m in normal tissue (182 ± 48 Ω·cm) and 0.67 – 0.99 S/m for infarcted tissue (125 ± 24 Ω·cm). Note that these values were measured 2 months after producing the infarction,[14] and hence we could assume that the infarcted tissue did not include fat. It should also be noted that these values correspond with the electrical conductivity globally measured in the tissue (and suggest that infarcted tissue is electrically more conductive than normal tissue). In contrast, when we model the infarcted zone as a mixture of normal tissue (viable myocardium), fibrosis and fat, the infarcted zone is expected to be less conductive than normal tissue, since fibrosis and fat are less conductive than normal tissue (see values in Table 1).

Results

Figure 2A shows the temperature distribution corresponding with the spatial distribution of tissues shown in Fig. 1B. The lesion depth (D) was 4.8 mm, surface width (SW) 8.0 mm, and maximum width (MW) 10.4 mm. The lesion in the case of assuming a myocardium comprised exclusively of healthy tissue was slightly deeper (D=5.0 mm) but narrower (SW=7.5 mm, MW=8.8 mm). The maximum temperature reached in the tissue was higher in the case of healthy tissue (97ºC vs. 85ºC) while the impedance was lower (79 Ω vs. 84 Ω). Figure 2B shows the distribution of current density in a selected zone. It is clearly

observed that electrical current flows preferentially through the tissues with higher electrical conductivity, i.e. through fibrous tissue versus fat, and through the viable myocardium versus fibrous tissue. The role of fat as an electrical insulator suggests that specific tissue distributions could significantly impact the performance of RF ablation on scar-related ventricular tachycardia either by enhancing this process (i.e., increasing the capability to create deeper lesions) or by worsening it (i.e., impeding the creation of deeper lesions).

To examine this, the original spatial tissue distribution shown in Fig. 1B was selectively modified to create 2 new spatial distributions, *tunneled* (Fig. 3A) and *blocking* (Fig. 3B). These distributions are two specific examples of possible infinite distributions even though they may appear somewhat arbitrary. We consider them relevant in the context of this study, since they represent two extreme cases in terms of favoring or preventing the passage of RF current through specific tissues. The *tunneled* distribution was intended to run RF current straightforwardly towards depth, and hence to explore an optimal scenario for creating a deeper thermal lesion. For this, two spatial modifications were implemented as described in Fig. 3. Conversely, the *blocking* distribution was aimed at impeding RF current from flowing preferentially towards depth. This was done by inserting a zone of fibrosis just under the electrode. Since fibrotic tissue is electrically less conductive than viable myocardium, this distribution would represent a possible situation in which it is potentially more difficult to create a deep thermal lesion. Figure 4A and 4B show the resultant temperatures for these new distributions. The *tunneled* distribution clearly favored a deeper (D=6.1 mm) but narrower (SW=7.8 mm, MW=10.2 mm) lesion. In contrast, the *blocked* distribution yielded a reduction in lesion depth (D= 4.7 mm) with similar lesion

width (SW=7.9 mm and MW=10.2 mm).

We analyzed in detail the spatial distributions of each term contributing to the total heating (Joule heating caused by RF power, thermal conduction, and blood perfusion). We observed that the small regions with high current density (associated with zones of high electrical conductivity) increase their temperature by Joule heating and then quickly heat neighboring tissue, regardless of the different thermal properties of the neighboring tissue (fat or fibrotic tissue). This is possibly the mechanism by which temperature spread out compared to the size of the heterogeneities.

Figure 5 shows temperature progress computed at subendocardial (3 mm deep) and intramural (6 mm deep) depths for normal and infarcted myocardium. Temperatures in the infarcted tissue were always greater than the normal tissue, which is consistent with prior ex vivo experiments.[2] When we simulated the range limits of electrical conductivity for normal and infarcted tissue, temperature progresses partially overlapped. Figure 6 illustrates the temperature profiles computed along the axis for the range limits of electrical conductivity for normal and infarcted tissue. The lesion depths were between 4.00 and 4.65 mm in the normal tissue and between 4.48 and 5.25 mm in the infarcted tissue.

Discussion

In this computational study, we created a computer model inspired by natural distributions of different tissue types represented in a ventricular infarct model. The results demonstrate that spatial distributions of different tissue types significantly alter the density of electrical current largely as a result of fat impeding the passage of current. However, the thermal lesions appear minimally unaffected by this phenomenon, with variations in depth of ~1

mm. However, one may assume that under extreme circumstances, fat and healthy myocardium could create preferential paths for electrical current within the scar that could hypothetically alter the lesion geometry. The lower maximum temperature reached in the scarred versus healthy tissue would suggest that more power may be delivered thereby enhancing the thermal lesion. Having said that, when we simulated an RF ablation on scarred tissue, increasing the power up from 12 W to 15 W (maximum power while maintaining the temperature below 100ºC) the lesion depth increased by a mere 0.3 mm.

The computer modeling results mimicking the ex vivo study by Kottkamp et al[2] were in fine agreement with these authors' experimental results. Although we found that temperatures in the infarcted tissue were always higher than the normal tissue, the sensitivity analysis varying the electrical conductivities of normal and infarcted tissue revealed that temperature progresses partially overlapped. Although Kottkamp et al[2] did not report thermal lesion sizes, our results (Figure 6) indicate that lesion depths created in normal tissue (4.00–4.65 mm) overlap those created in infarcted tissue (4.48–5.25 mm), which is also in agreement with that reported by Kovoor et al,[3] who did not find differences in lesion size between normal and scarred tissue.

It is important to emphasize that our model only takes into account passive electrical properties of the tissue. As such, our model was not defined in terms of electrical conduction of action potentials (e.g. slowly-conducting pathways vs. normally-conducting tissue), but it was based upon histology (i.e., viable myocardium, vs. fibrous tissue vs. fat). In spite of this limitation, the proposed model is still deemed appropriate since creation of thermal lesions is in general governed by passive electrical tissue characteristics.

Conclusions

The findings of this computational model suggest that while during RF ablation of scar-related ventricular tachycardia differences in tissue characteristics may affect the density of electrical current, overall this does not appear to significantly impact the size of the created thermal lesions. Thus, one may assume that tissue type or characteristic does not appreciably influence the outcomes of RF catheter ablation of scar-related VT.

Author contributions: JJP and MT: Building of the model, data analysis/interpretation; AA, AA and EB: Concept/design, drafting article. All authors: critical Revision and approval of article.

References

1. Aryana A, d'Avila A. Contact force during VT ablation: vector orientation is key. Circ Arrhythm Electrophysiol. 2014;7:1009-10.
2. Kottkamp H, Hindricks G, Horst E, Baal T, Fechtrup C, Breithardt G, Borggrefe M. Subendocardial and intramural temperature response during radiofrequency catheter ablation in chronic myocardial infarction and normal myocardium. Circulation. 1997;95:2155-61.
3. Kovoor P, Daly MP, Pouliopoulos J, Byth K, Dewsnap BI, Eipper VE, Yung T, Uther JF, Ross DL. Comparison of radiofrequency ablation in normal versus scarred myocardium. J Cardiovasc Electrophysiol. 2006;17:80-6.
4. Betensky BP, Jauregui M, Campos B, Michele J, Marchlinski FE, Oley L, Wylie B, Robinson D, Gerstenfeld EP. Use of a novel endoscopic catheter for direct visualization and ablation in an ovine model of chronic myocardial infarction. Circulation. 2012;126:2065-72.
5. Sasaki T, Calkins H, Miller CF, Zviman MM, Zipunnikov V, Arai T, Sawabe M, Terashima M, Marine JE, Berger RD, Nazarian S, Zimmerman SL. New insight into scar-related ventricular

tachycardia circuits in ischemic cardiomyopathy: Fat deposition after myocardial infarction on computed tomography--A pilot study. Heart Rhythm. 2015;12:1508-18.

6. Goldfarb JW, Roth M, Han J. Myocardial fat deposition after left ventricular myocardial infarction: assessment by using MR water-fat separation imaging. Radiology. 2009;253:65-73.
7. Ichikawa Y, Kitagawa K, Chino S, Ishida M, Matsuoka K, Tanigawa T, Nakamura T, Hirano T, Takeda K, Sakuma H. Adipose tissue detected by multislice computed tomography in patients after myocardial infarction. JACC Cardiovasc Imaging. 2009;2:548-55.
8. Su L, Siegel JE, Fishbein MC. Adipose tissue in myocardial infarction. Cardiovasc Pathol. 2004;13:98-102.
9. Suárez AG, Hornero F, Berjano EJ. Mathematical modeling of epicardial RF ablation of atrial tissue with overlying epicardial fat. Open Biomed Eng J. 2010;4:47-55.
10. Pérez JJ, D'Avila A, Aryana A, Berjano E. Electrical and thermal effects of esophageal temperature probes on radiofrequency catheter ablation of atrial fibrillation: results from a computational modeling study. J Cardiovasc Electrophysiol. 2015;26:556-64.
11. Berjano EJ. Theoretical modeling for radiofrequency ablation: state-of-the-art and challenges for the future. Biomed Eng Online. 2006;5:24.
12. Hasgall PA, Di Gennaro F, Baumgartner C, Neufeld E, Gosselin MC, Payne D, Klingenböck A, Kuster N, “IT’IS Database for thermal and electromagnetic parameters of biological tissues,” Version 3.0, September 01st, 2015, DOI: 10.13099/VIP21000-03-0. www.itis.ethz.ch/database
13. Gonzalez-Suarez A, Berjano E. Comparative analysis of different methods of modeling the thermal effect of circulating blood flow during RF cardiac ablation. IEEE Trans Biomed Eng. 2015 Jul 31. [Epub ahead of print]
14. Salazar Y, Bragos R, Casas O, Cinca J, Rosell J. Transmural versus nontransmural in situ electrical impedance spectrum for healthy, ischemic, and healed myocardium. IEEE Trans Biomed Eng. 2004;5:1421-7.

Table 1 Physical characteristics of tissues and materials employed in the computational model.[10,12,13]

Tissue	σ (S/m)	k (W/m·K)	ρ (kg/m^3)	c (J/kg·K)	ω_b (1/s)
Fat [12]	0.044	0.21	911	2348	0.0005
Viable myocardium [12]	0.6	0.54	1060	3111	0.018
Fibrotic tissue [12]	0.4	0.39	1027	2372	0.0006
Connective tissue [10]	0.09	0.4	3200	1000	#
Cardiac chamber/Blood [12]	0.99	0.54	1000	4180	
Electrode/Pt-Ir [13]	4.6×10^6	71	21500	132	
Catheter/Polyurethane [13]	10^{-5}	0.026	70	1045	

σ: electric conductivity; k: thermal conductivity; ρ: density; c: specific heat; ω_b: blood perfusion.

[#] Blood perfusion in the connective tissue was discarded due to its low value compared to the cardiac tissue (37 vs. 1026 ml/min/kg).[12]

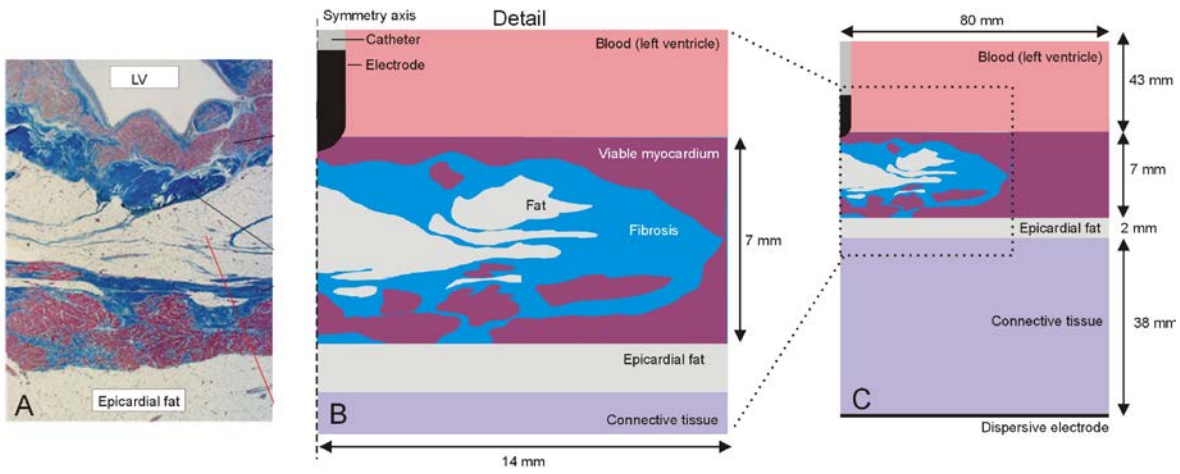

Figure 1 **A:** Histological image showing the constituent tissues in a scar within the ventricular wall: viable myocardium, fibrous tissue and fat (reproduced with permission from Sasaki et al 2015. Copyright 2015, Elsevier). Since fat serves as an electrical insulator, both scar and fat may support low conduction paths in scar-related ventricular tachycardia. **B:** Detail of the computer model showing the spatial distribution of these types of tissues inspired by the histological image, along with an irrigated electrode perpendicularly placed on the endocardium. **C:** Overview of the computer model showing the location of the dispersive electrode on the bottom surface. (Only electrode tip and detail of the ventricular wall are to scale).

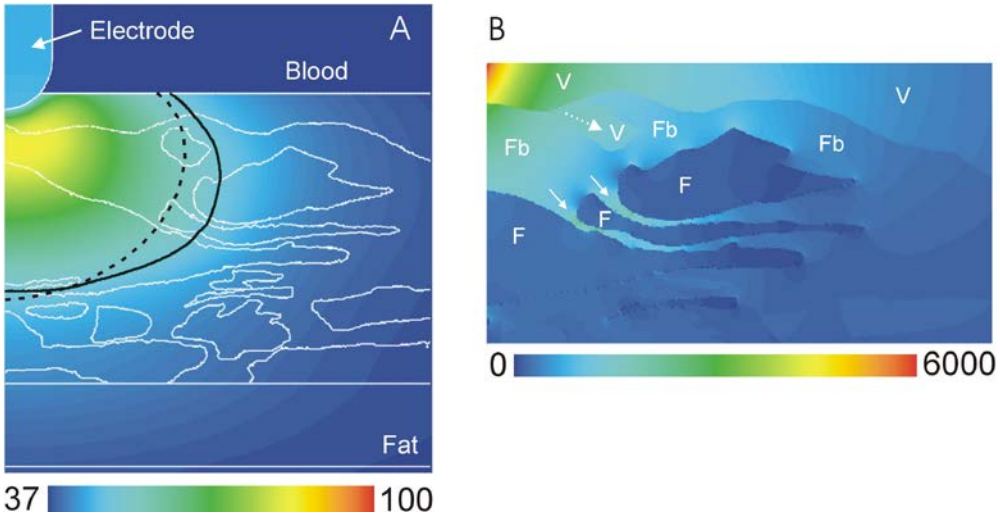

Figure 2 **A:** Computed temperature distribution (ºC) in the ventricular wall shown in Fig. 1B. Black line corresponds to the 50ºC isotherm and represents the thermal lesion boundary. (For comparison, dashed line corresponds to the 50ºC isotherm in the case of a healthy myocardium) **B:** Current density distribution (A/m^2) in different tissues represented within the scar (F: fat; Fb: Fibrosis; V: Viable myocardium). The image is of a detailed area of the ventricular wall shown in **A**. Note that electrical current flows preferentially through tissues with higher electrical conductivity, i.e. through fibrous tissue instead of fat (solid arrows), and through viable myocardium instead of fibrous tissue (dashed arrow).

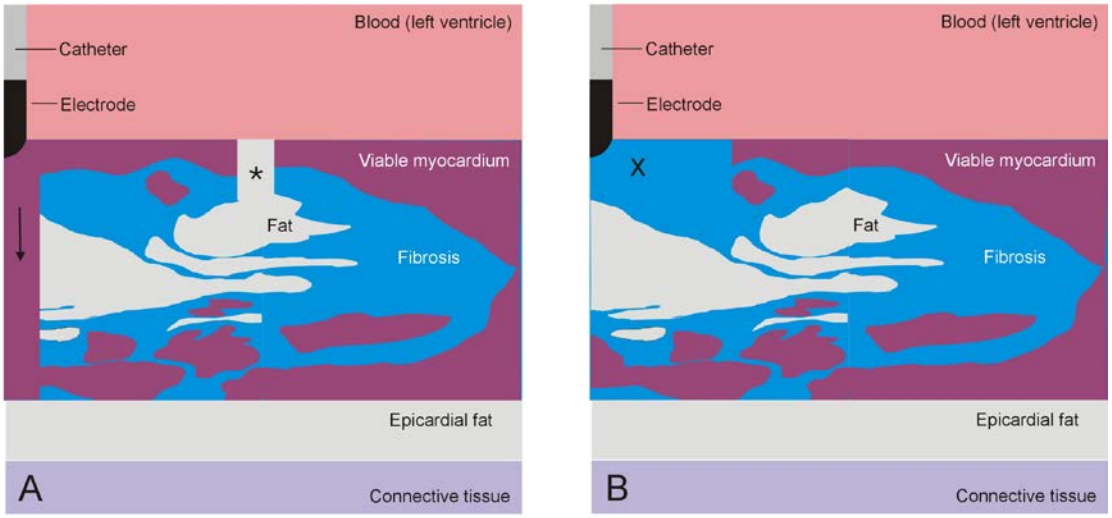

Figure 3 Modifications on the original distribution of tissues shown in Fig. 1B. These modifications were aimed at exploring how the insulation effect exerted by fat alters the electrical and thermal performance of RF ablation. In **A** (*tunneled*), two changes were implemented: 1) a fragment of fat (*) was placed in a zone previously occupied by viable myocardium and where current density was observed to be very high (see Fig. 2); and 2) a new fragment of viable myocardium (arrow) was placed just below the electrode, and passed through all the zones previously occupied by fat which was observed to impede the flow of electrical current (see Fig. 2). In **B** (*blocked*), the zone of viable myocardium previously located just below the electrode was replaced by a zone of fibrosis (×).

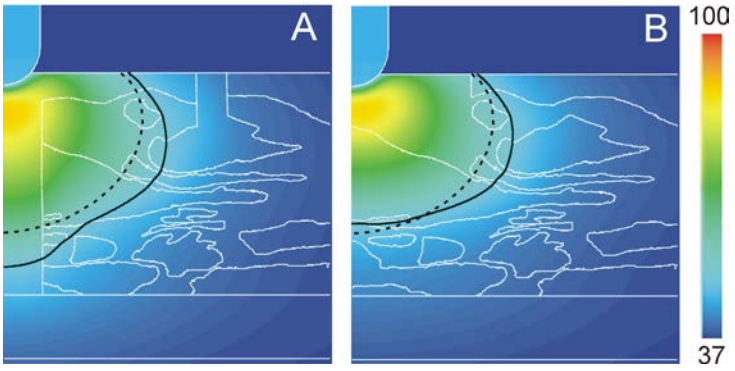

Figure 4 **A** and **B:** Computed temperature distribution (ºC) corresponding with spatial distributions shown in Fig. 3. Black line corresponds with the 50ºC isotherm and represents the thermal lesion boundary. (For comparison, dashed line corresponds with the 50ºC isotherm in the case of a myocardium completely healthy).

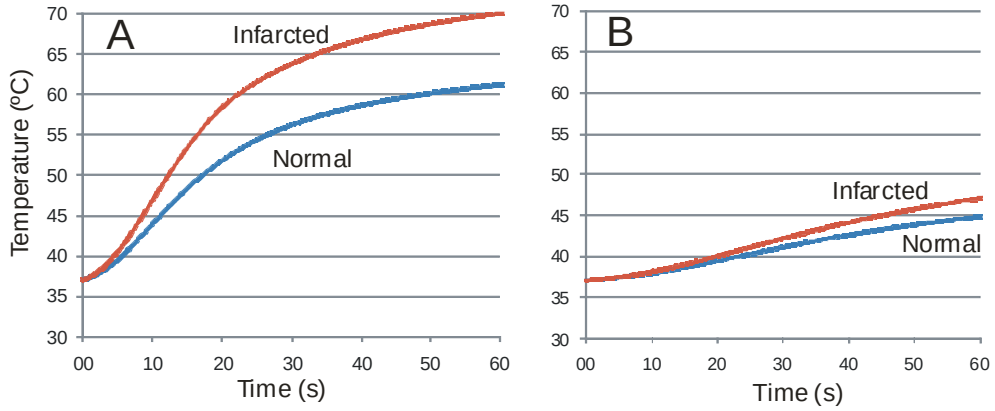

Figure 5 Temperature progress computed at 3 mm depth (**A**) and 6 mm depth (**B**) for mean values of electrical conductivity of normal and infarcted myocardium during RF ablation mimicking the studies by Kottkamp et al.[2]

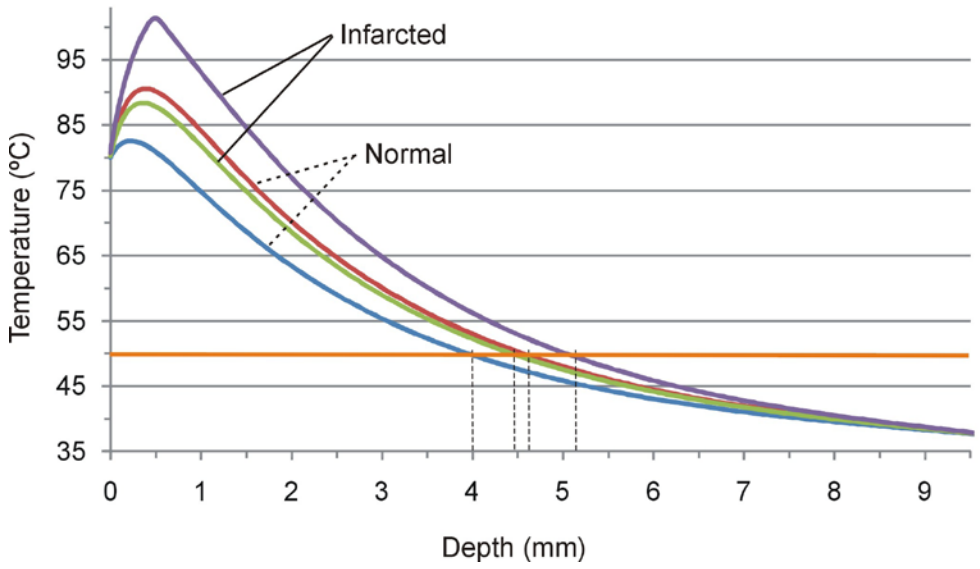

Figure 6 Temperature profiles across the symmetry axis for the mean values of electrical conductivity of normal and infarcted myocardium at the end of 60 s of RF ablation mimicking the studies by Kottkamp et al.[2]